Identification of DPY19L3 as the *C*-mannosyltransferase of R-spondin1 in human cells

Yuki Niwa[a], Takehiro Suzuki[b], Naoshi Dohmae[b], and Siro Simizu[a,*]
[a]Department of Applied Chemistry, Faculty of Science and Technology, Keio University, Yokohama 223-8522, Japan;
[b]Biomolecular Characterization Unit, RIKEN Center for Sustainable Resource Science, Wako 351-0198, Japan

ABSTRACT **R-spondin1 (Rspo1) is a secreted protein that enhances Wnt signaling, which has crucial functions in embryonic development and several cancers. *C*-mannosylation is a rare type of glycosylation and might regulate secretion, protein–protein interactions, and enzymatic activity. Although human Rspo1 contains 2 predicted *C*-mannosylation sites, *C*-mannosylation of Rspo1 has not been reported, nor have its functional effects on this protein. In this study, we demonstrate by mass spectrometry that Rspo1 is *C*-mannosylated at W^{153} and W^{156}. Using Lec15.2 cells, which lack dolichol-phosphate-mannose synthesis activity, and mutant Rspo1-expressing cells that replace W^{153} and W^{156} by alanine residues, we observed that *C*-mannosylation of Rspo1 is required for its secretion. Further, the enhancement of canonical Wnt signaling by Rspo1 is regulated by *C*-mannosylation. Recently DPY19 was reported to be a *C*-mannosyltransferase in *Caenorhabditis elegans*, but no *C*-mannosyltransferases have been identified in any other organism. In gain- and loss-of-function experiments, human DPY19L3 selectively modified Rspo1 at W^{156} but not W^{153} based on mass spectrometry. Moreover, knockdown of DPY19L3 inhibited the secretion of Rspo1. In conclusion, we identified DPY19L3 as the *C*-mannosyltransferase of Rspo1 at W^{156} and found that DPY19L3-mediated *C*-mannosylation of Rspo1 at W^{156} is required for its secretion.**

Monitoring Editor
Akihiko Nakano
RIKEN

Received: Jun 15, 2015
Revised: Jan 4, 2016
Accepted: Jan 5, 2016

INTRODUCTION

Wnt signaling has critical functions in embryonic development and cell proliferation, survival, and migration (Anastas and Moon, 2013). Abnormal Wnt signaling has been implicated in various diseases, including colon cancer and melanoma (Niehrs, 2012). R-spondins (Rspos), identified in 2004 (Kamata *et al.*, 2004), enhance Wnt signaling with Wnts synergistically (Kazanskaya *et al.*, 2004; Kim *et al.*, 2008; Schuijers and Clevers, 2012). Rspos are growth factors for intestinal crypt stem cells in vivo (Kim *et al.*, 2005), and a loss-of-function mutation of Rspo1 develops into a recessive syndrome characterized by XX sex reversal (Parma, Radi, *et al.*, 2006). Further, aberrant expression of Rspos promotes tumor malignancy (Carmon *et al.*, 2014; Shinmura *et al.*, 2014; Gong *et al.*, 2015; Ilmer *et al.*, 2015).

The human Rspo family comprises four members (Rspo1–4), which share 40–60% amino acid sequence homology (Kim *et al.*, 2006). All Rspo proteins have two furin (Fu) repeats at the N-terminus, followed by one thrombospondin type 1 repeat (TSR1) and a basic C-terminal tail. Rspos bind their receptors—the leucine-rich repeat–containing G protein–coupled receptors (LGRs) 4–6 and zinc and ring finger 3 or its homologue, ring finger 43 (RNF43)—through two Fu domains (de Lau, Barker, *et al.*, 2011; Glinka, Dolde, Kirsch, Huang, *et al.*, 2011; Hao, Xie, *et al.*, 2012; Wang *et al.*, 2013), and the ternary complex crystal structure of Rspo1-LGR5-RNF43 has been reported (Chen *et al.*, 2013). Thus the two Fu domains of Rspo1 are essential for enhancing Wnt signaling (Kazanskaya *et al.*, 2004; Nam *et al.*, 2006; Kim *et al.*, 2008). In contrast, the TSR1 and C-terminal region of Rspos are necessary for binding heparan sulfate proteoglycan (HSPG; Nam *et al.*, 2006; Carlson *et al.*, 2008), but the significance of these regions in Wnt signaling remains obscure.

This article was published online ahead of print in MBoC in Press (http://www.molbiolcell.org/cgi/doi/10.1091/mbc.E15-06-0373) on January 13, 2016.

*Address correspondence to: Siro Simizu (simizu@applc.keio.ac.jp).

Abbreviations used: CBB, Coomassie brilliant blue; Dol-P-Man, dolichol-phosphate-mannose; ER, endoplasmic reticulum; Fu, furin; HSPG, heparan sulfate proteoglycan; LGR, leucine-rich repeat–containing, G protein–coupled receptor; MH, myc-hexahistidine; RNF43, ring finger 43; Rspo, R-spondin; TSR1, thrombospondin type 1 repeat.

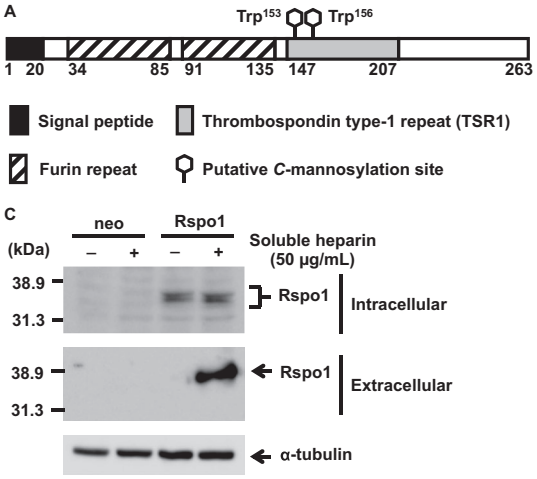

FIGURE 1: Establishment of an Rspo1-overexpressing cell line. (A) Schematic of human Rspo1. Rspo1 has two predicted *C*-mannosylation sites in the TSR1. The black box, two hatched bars, gray box, and two hexagonal shapes denote the signal peptide, furin repeats, TSR1, and putative *C*-mannosylation sites, respectively. (B) Amino acid sequence homology between human Rspo1-4 and mouse Rspo1. Two putative *C*-mannosylation sites are conserved in all Rspos. Conserved amino acids are indicated by asterisks, and putative *C*-mannosyltryptophan residues are underlined. (C) Rspo1 binds to cell surface HSPGs. Each cell line was cultured with or without 50 μg/ml soluble heparin, and all lysates and conditioned media were electrophoresed and immunoblotted with anti–c-myc and anti–α-tubulin. Rspo1 was secreted only after treatment with soluble heparin.

C-mannosylation is a posttranslational modification of the first tryptophan residue in the consensus sequence W-X-X-W/C (in which X represents any amino acid) by an endoplasmic reticulum (ER)–localized enzyme (Krieg *et al.*, 1998; Julenius, 2007). *C*-mannosylation was first reported in ribonuclease 2 (Hofsteenge *et al.*, 1994), but *C*-mannosylated proteins are sorted primarily into two groups: TSR1-containing proteins, such as thrombospondin-1 (Hofsteenge *et al.*, 2001), and type I cytokine receptors that contain a W-S-X-W-S motif, such as interleukin-21 receptor (Hamming *et al.*, 2012). Several studies suggested that *C*-mannosylation is important for protein–protein interactions (Ihara *et al.*, 2010; Hamming *et al.*, 2012); however, the direct effect of *C*-mannosylation on protein function is poorly understood. DPY19 was reported to be the *C*-mannosyltransferase of the TSR1 peptide in *Caenorhabditis elegans* (Buettner *et al.*, 2013), but no enzymes that catalyze *C*-mannosylation have been identified in any other organism. Humans have four homologues of *C. elegans* DPY19: DPY19L1–L4. Thus human DPY19L1–L4 are likely to be *C*-mannosyltransferases, although this has not been demonstrated experimentally.

Human Rspo1 has two predicted *C*-mannosylation sites (W^{153} and W^{156}) in the TSR1, but whether Rspo1 is *C*-mannosylated has not been reported. In this study, we demonstrate that Rspo1 is *C*-mannosylated at W^{153} and W^{156} and that *C*-mannosylation of Rspo1 regulates its secretion and canonical Wnt/β-catenin signaling. Further, we also provide evidence that human DPY19L3 is the *C*-mannosyltransferase of Rspo1 at W^{156} and that DPY19L3-mediated *C*-mannosylation of Rspo1 governs its secretion.

RESULTS

C-mannosylation of Rspo1 at W^{153} and W^{156}

Human Rspo1 has two predicted *C*-mannosylation consensus sequences—W^{153} (W^{153}-S-P-W) and W^{156} (W^{156}-G-P-C)—in the TSR1 (Figure 1, A and B). Because *C*-mannosylation consensus sequences are conserved in human Rspo1–4 and mouse Rspos (Figure 1B), *C*-mannosylation of Rspos might regulate their functions. To determine whether Rspo1 is *C*-mannosylated, we used a C-terminal myc-hexahistidine (MH)–tagged Rspo1-overexpressing HT1080 cell line, HT1080-Rspo1-MH cells (Tsuchiya *et al.*, 2016). In an earlier study, Rspo1 bound to cell surface HSPGs and was secreted into conditioned medium after cells were treated with soluble heparin (Nam *et al.*, 2006). We also noted secreted Rspo1 only after treatment with soluble heparin of the cells (Figure 1C).

To determine whether Rspo1 is *C*-mannosylated, we purified recombinant Rspo1 protein from the conditioned medium of HT1080-Rspo1-MH cells for liquid chromatography–mass spectrometry (LC-MS) analysis (Figure 2). HT1080-Rspo1-MH cells were cultured in serum-free medium with soluble heparin for 24 h, and recombinant Rspo1 was purified using Ni– nitriloacetic acid (NTA) agarose (Figure 2A). Purified Rspo1 was digested with trypsin and Asp-N, and the resulting mixture of peptides was analyzed by LC-MS. The doubly charged form of the peptide ^{152}EWSPWGPCSK^{161} has m/z = 624.27, which is the predicted mass of unmannosylated peptide, and no signal was derived from the unmannosylated peptide; however, the doubly charged form of ^{152}EWSPWGPCSK^{161} to which two mannose residues have been added has m/z = 786.33, and a signal of m/z = 786.33 was observed at 9.97 min in the chromatogram (Figure 2B). These data suggest that Rspo1 is *C*-mannosylated at W^{153} and W^{156}.

To confirm the sequence of the ion and determine two *C*-mannosylation sites in Rspo1, we performed LC-MS/MS analysis (Figure 2C). Addition of 162 Da (one mannose residue) was observed in the y_7 and y_8 ions but not the y_1–y_5 ions, indicating this modification occurred at P^{155} or W^{156}. Similarly, the other modification occurred at E^{152} or W^{153}. Glycosylation at P and E residues was not reported previously, and the W^{153} and W^{156} residues meet the *C*-mannosylation consensus sequence W-X-X-W/C, suggesting that Rspo1 is *C*-mannosylated at W^{153} and W^{156}. Further, characteristic cross-ring cleavages of *C*-mannose, resulting in losses of 120 Da (Hofsteenge *et al.*, 1994), were observed in the y_7 and y_8 but not the y_1–y_5 ions. These findings also suggested that Rspo1 is *C*-mannosylated at W^{153} and W^{156}. We also observed that ~10% of Rspo1 was mono-*C*-mannosylated by LC-MS (Figure 2D), and LC-MS/MS analysis suggested that this modification occurred only at W^{153} (Figure 2E); there was no mono-*C*-mannosylation of W^{156} in the conditioned medium by LC-MS/MS. Thus all secreted Rspo1 was *C*-mannosylated, and most Rspo1 was *C*-mannosylated at both W^{153} and W^{156}; some mono-*C*-mannosylation occurred only at W^{153}.

C-mannosylation of Rspo1 regulates its secretion

Previous reports demonstrated that *C*-mannosylation uses dolichol-phosphate-mannose (Dol-P-Man) as the mannose donor, and Lec15.2 cells, a CHO-K1 cell subline, lack Dol-P-Man synthesis activity, resulting in a *C*-mannosylation defect (Camp *et al.*, 1993; Doucey *et al.*, 1998; Wang *et al.*, 2009). By using CHO-K1 and Lec15.2 cells, we first analyzed the effect of *C*-mannosylation on the secretion of Rspo1. It has been reported that deficiency of Dol-P-Man synthesis affects *N*-glycosylation (Lehrman and Zeng, 1989;

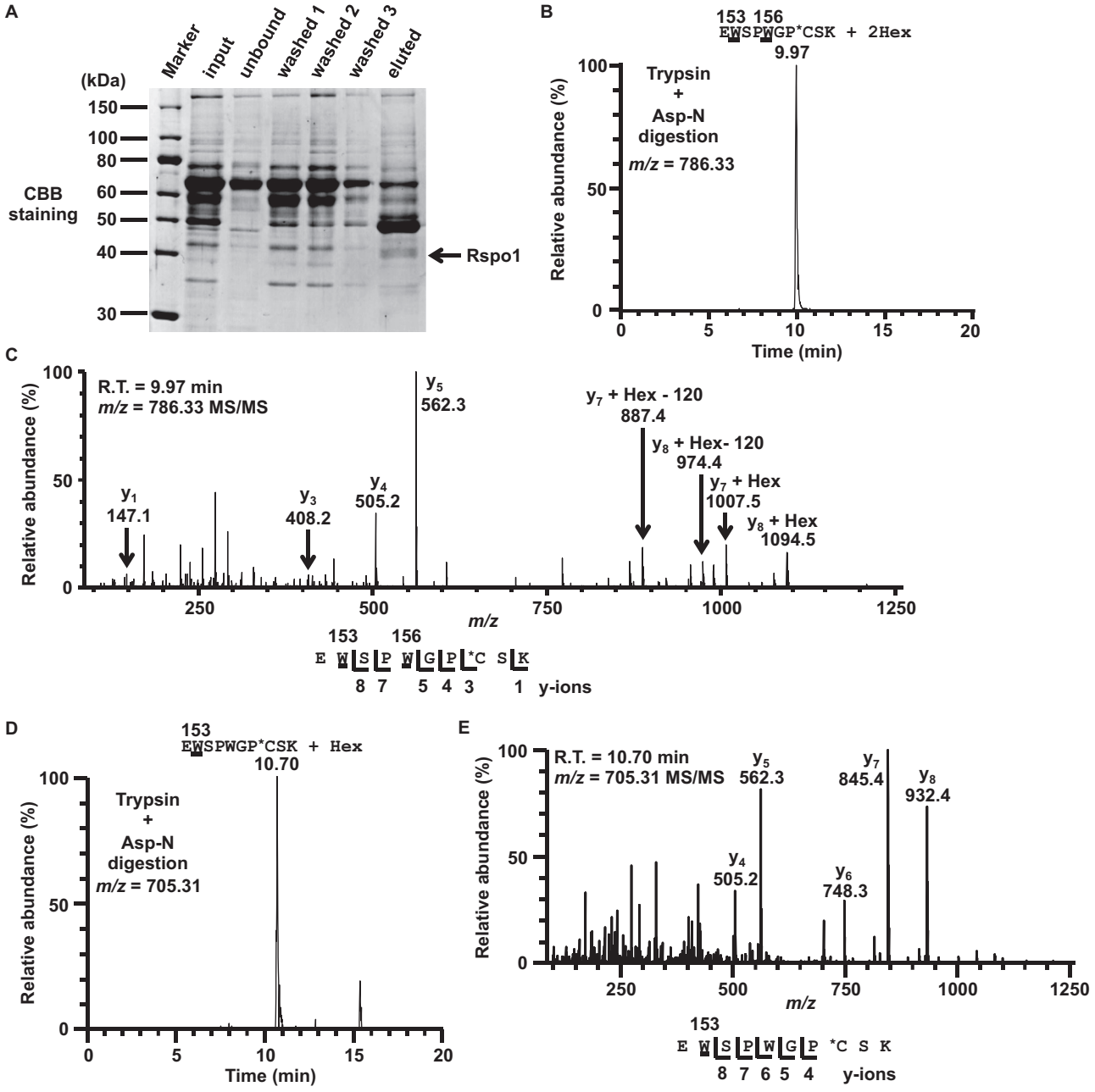

FIGURE 2: Identification of *C*-mannosylation sites in Rspo1. (A) Separation of recombinant Rspo1 from the conditioned medium of HT1080-Rspo1-MH cells. Secreted Rspo1-MH was purified with Ni-NTA agarose, and samples were electrophoresed on an SDS–polyacrylamide gel. The gel was visualized with CBB staining. (B–E) Identification of *C*-mannosylation sites in Rspo1. Samples were digested with trypsin and Asp-N, and the resulting peptides were analyzed by LC-MS/MS. The signal was observed in the chromatogram at $m/z = 786.33$ (B) and 705.31 (D). The ions at 9.97 min ($m/z = 786.33$) and 10.70 min ($m/z = 705.31$) were further analyzed by LC-MS/MS, respectively (C, E). Indicated *y* ions were detected, and both W^{153} and W^{156} (C) or only W^{153} (E) of Rspo1 was *C*-mannosylated. *C*-mannosylation sites are underlined. *C, propionamide cysteine.

Zeng and Lehrman, 1990), and our previous work demonstrated that *N*-glycosylation of Rspo1 at N^{137} negatively regulates its secretion (Tsuchiya *et al.*, 2016). To exclude the effect of *N*-glycosylation of Rspo1, we used a mutant form of Rspo1 in which an asparagine residue is replaced by a glutamine residue (N137Q; Tsuchiya *et al.*, 2016). Parental CHO-K1 or Lec15.2 cells were transiently transfected with Rspo1/N137Q, and the amount of secreted Rspo1 was evaluated. For Lec15.2 cells, inhibition of *C*-mannosylation of Rspo1/N137Q reduced the secreted level of Rspo1/N137Q, concomitant with an increase of intracellular Rspo1/N137Q, compared with the parental CHO-K1 cells (Figure 3A). These results suggested that *C*-mannosylation of Rspo1 regulates its secretion.

Next we constructed a mutant form of Rspo1 in which tryptophan residues were replaced by alanine residues (W153A/W156A: 2WA) and established Rspo1/2WA-overexpressing HT1080 cells, termed HT1080-Rspo1/2WA-MH cells. Equal amounts of exogenous Rspo1

in these cells were confirmed by Western blot and reverse transcription (RT)-PCR (Figure 3, B and C). Using these cell lines, we first measured the effects of *C*-mannosylation on intracellular trafficking. Wild-type Rspo1 barely colocalized with KDEL, an ER marker, with which Rspo1/2WA partially colocalized (Figure 3D). In the Golgi apparatus, both wild-type and 2WA mutant Rspo1 colocalized with GRASP65, a Golgi marker (Figure 3E). These data suggest that *C*-mannosylation of Rspo1 contributes to its transport from the ER to the Golgi apparatus.

Among TSR1-containing proteins, punctin-1 is *C*-mannosylated, and *C*-mannosylation of punctin-1 is required for its secretion (Wang *et al.*, 2009). Rspo1/2WA decreased its secretion and accumulated in cells simultaneously compared with wild-type Rspo1 (Figure 3F), which agrees with results of using CHO-K1 and Lec15.2 cells (Figure 3A). Furthermore, during the time-course experiment, the amount of secreted Rspo1/2WA was lower than that of wild-type Rspo1 (Figure 3G). Thus these results indicate that *C*-mannosylation of Rspo1 regulates the kinetics of its secretion.

C-mannosylation of Rspo1 enhances canonical Wnt signaling

Because Rspo1 increases Wnt signaling with Wnts synergistically (Kim *et al.*, 2008; Glinka, Dolde, Kirsch, Huang, *et al.*, 2011), we examined whether *C*-mannosylation of Rspo1 affects this enhancement. *C*-mannosylation of Rspo1 regulates the kinetics of its secretion, and the levels of 2WA mutant Rspo1 in conditioned medium are lower than wild-type Rspo1 (Figure 3, F and G); thus we purified wild-type and the 2WA mutant Rspo1 from conditioned media of each culture, and used equal amounts of each protein for stimulation (Figure 3H, inset). To measure the activation of Wnt signaling, we transfected TOPFlash, which is a canonical Wnt signaling reporter and has tandem TCF/LEF-binding sites upstream of a firefly luciferase reporter, or the mutant reporter FOPFlash into 293T cells, which were then treated with Wnt3a-conditioned medium and each Rspo1 protein, and luciferase activities were measured. Wild-type Rspo1 increased TOPFlash activity by 20-fold, compared to 2.5-fold by Rspo1/2WA (Figure 3H). This suggests that *C*-mannosylation of Rspo1 in part mediates the enhancement in canonical Wnt signaling.

Identification of DPY19L3 as the *C*-mannosyltransferase of Rspo1 at W^{156}

DPY19 was identified as a *C*-mannosyltransferase that glycosylates TSR1 in *C. elegans* (Buettner *et al.*, 2013); however, no enzymes that catalyze *C*-mannosylation have been identified in any other organism. Because *C*-mannosylation of Rspo1 occurs in TSR1 (Figure 1A) and because there are four human homologues of DPY19 (DPY19L1-L4), we hypothesized that at least one of them is a *C*-mannosyltransferase of Rspo1. To identify the *C*-mannosyltransferase(s) of Rspo1, we performed gain-of-function experiments.

Drosophila S2 cells have no *C*-mannosyltransferase activity (Krieg, Gläsner, *et al.*, 1997; Hofsteenge *et al.*, 2001; Buettner *et al.*, 2013) but harbor Dol-P-Man, which is the donor substrate for *C*-mannosylation. We established five S2 cell lines that expressed human DPY19L1-L4 or empty vector (mock), respectively, and confirmed the expression of each of (Figure 4A, inset). Human Rspo1 cDNA was transiently transfected into each S2 cell line, and recombinant Rspo1 proteins were purified from each S2 cell culture medium. Purified Rspo1 was analyzed by LC-MS. Monomannosylated peptide was observed only when the protein was produced in DPY19L3-expressing S2 cells (Figure 4A). Dimannosylated peptide was not observed in any sample (Figure 4A). These results suggested that human DPY19L3 catalyzes *C*-mannosylation of human Rspo1. To determine the *C*-mannosylation site, we analyzed unmannosylated and monomannosylated peptides from DPY19L3-expressing S2 cells by LC-MS/MS (Figure 4B). Of note, the y_4 and y_5 ions corresponded well in both peptides, and the signal from the characteristic cross-ring cleavages were observed at the y_7 and y_8 ions in the monomannosylated peptide (Figure 4B), demonstrating that DPY19L3 modifies selectively at W^{156} but not W^{153} of Rspo1. Thus, using the S2 cell system, we can produce *C*-mannosylated Rspo1 at only the W^{156} residue. Empty vector (mock)–transfected S2 cells produce only nonmannosylated Rspo1; DPY19L3-expressing S2 cells produce nonmannosylated and W^{156}-mannosylated Rspo1 (Figure 4, A and B). We purified these Rspo1s from each culture medium and used an equal amount of each protein for stimulation (Figure 4C, inset). TOPFlash activity of 293T cells stimulated with Rspo1 produced by DPY19L3-expressing S2 cells was significantly increased compared with that by mock-transfected S2 cells (Figure 4C). These results supported that *C*-mannosylation of Rspo1 regulates the enhancing activity of Wnt signaling.

Next, to confirm that *C*-mannosylation of Rspo1 at W^{156} is catalyzed by DPY19L3 in human cells, we performed loss-of-function experiments in Rspo1-overexpressing HT1080 cells. DPY19L1, DPY19L3, and DPY19L4 were highly expressed, but DPY19L2 was barely detected in HT1080-Rspo1-MH cells (Figure 5A, top). Further, DPY19L2 mRNA levels were lower than the others (Figure 5A, bottom). DPY19L2 expression is restricted to testis in human (Dezső, Nikolsky, *et al.*, 2008), and many reports demonstrated the specific function of DPY19L2 in testis, the deletion of which is a major cause of globozoospermia (Harbuz *et al.*, 2011; Koscinski, Elinati, *et al.*, 2011). Moreover, from the result of gain-of-function experiments in S2 cells, DPY19L2 was not the *C*-mannosyltransferase for Rspo1 (Figure 4, A and B). On the basis of these results and reports, we believed that the low expression of DPY19L2 in HT1080-Rspo1-MH cells was most likely ectopic expression; thus we excluded the possibility that DPY19L2 might be a candidate *C*-mannosyltransferase for Rspo1 at W^{156}.

We depleted DPY19L1, DPY19L3, or DPY19L4 by small interfering RNA (siRNA) in HT1080-Rspo1-MH cells and analyzed the results by MS (Figure 5, B and C). The levels of each siRNA were measured by quantitative RT-PCR, and knockdown efficiencies were recorded for each siRNA of these target genes (Figure 5B). We purified Rspo1 from the conditioned medium of each siRNA-treated culture and analyzed it by matrix-assisted laser desorption/ionization time-of-flight (MALDI-TOF) MS and MS/MS. The signals that had masses that derived from dimannosylated (at both W^{153} and W^{156}) and monomannosylated (only at W^{153}) peptides were observed at approximately m/z = 1919 and 1757, respectively (Figure 5C). By MALDI-TOF MS analysis of siDPY19L1- and siDPY19L4-treated Rspo1 that was purified from the conditioned medium of each siRNA-treated culture, we determined that DPY19L1 and DPY19L4 were not *C*-mannosyltransferases of Rspo1, because both peptides (monomannosylated and dimannosylated) were still observed at nearly the same ratio compared with siCtrl-treated Rspo1 (Figure 5C, siCtrl vs. siDPY19L1 and siDPY19L4). In contrast, siDPY19L3-treated Rspo1 decreased the levels of dimannosylated peptide (at both W^{153} and W^{156}) and increased those of monomannosylated peptide (only at W^{153}; Figure 5C, siCtrl vs. siDPY19L3). Unmannosylated peptide (m/z = 1595) and monomannosylated peptide at W^{156} (m/z = 1757) were absent from all samples, including siDPY19L3-treated Rspo1, by MS/MS. Similar results were obtained for Rspo1 from DPY19L3-depleted cells using another siRNA against DPY19L3 (siDPY19L3#2) (unpublished data). These results demonstrated that

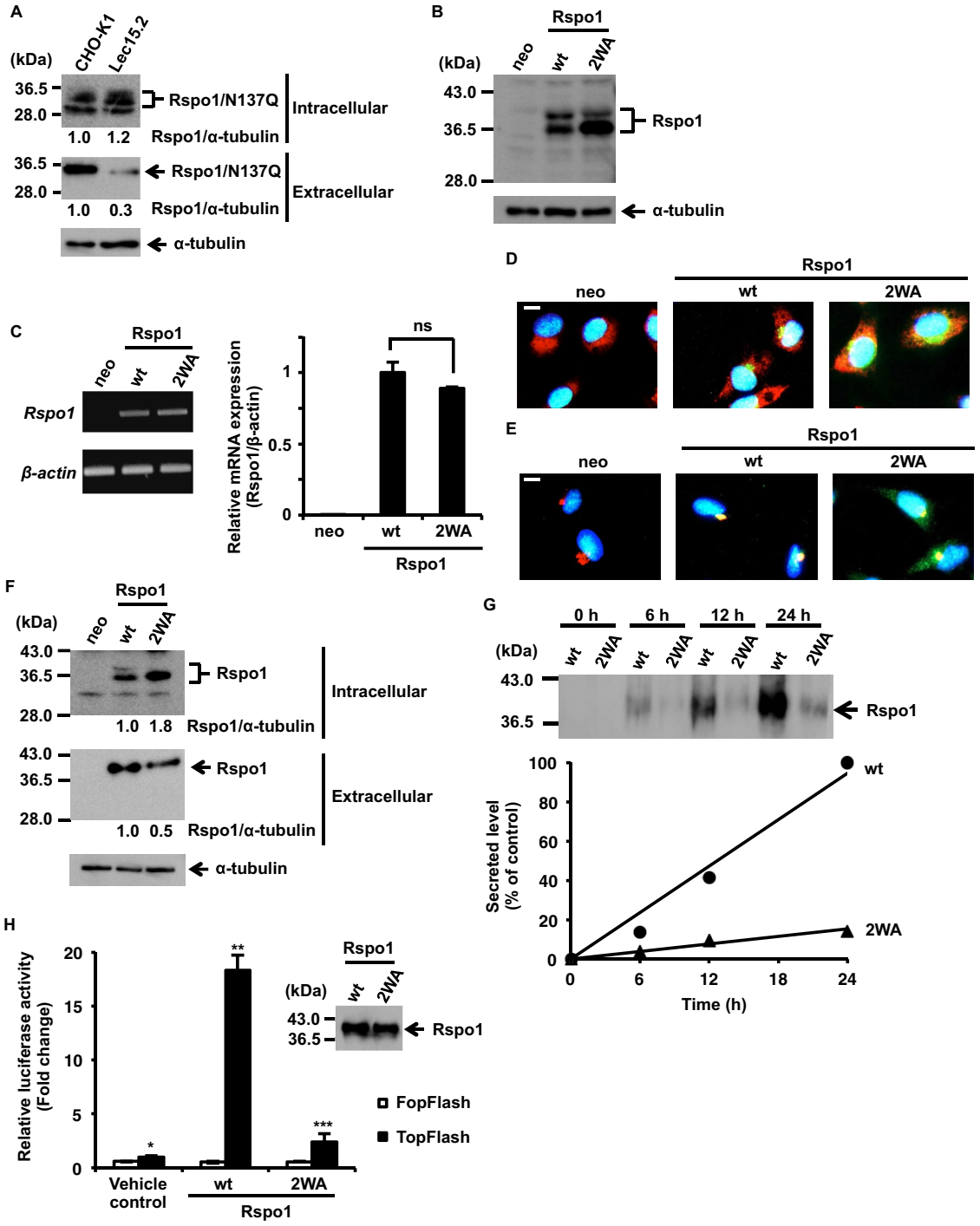

FIGURE 3: Effect of *C*-mannosylation on Rspo1 function. (A) Effect of *C*-mannosylation on Rspo1 secretion using CHO-K1 and Lec15.2 cells. CHO-K1 and Lec15.2 cells were transiently transfected with pCI-neo-Rspo1/N137Q-MH vector for 6 h and then cultured in serum-free medium with 50 μg/ml soluble heparin for 18 h. The protein samples were electrophoresed and immunoblotted with anti–c-myc and anti–α-tubulin. Signal intensities of Rspo1 were quantified and normalized to α-tubulin expression using ImageJ software. The Rspo1/α-tubulin ratio (CHO-K1) was defined as 1.0. (B, C) Establishment of mutant form of Rspo1 (W^{153} and W^{156} replaced by alanine residues; W153A/W156A: 2WA)–overexpressing HT1080 cell line, HT1080-Rspo1/2WA-MH. HT1080-neo (neo), HT1080-Rspo1-MH (wt), and HT1080-Rspo1/2WA-MH (2WA) cells were lysed, and aliquots of the cell lysates were electrophoresed and immunoblotted with anti–c-myc and anti–α-tubulin (B). Total RNA was isolated from each cell line, and semiquantitative (left) and quantitative (right) RT-PCR was performed (C). Equal amounts of exogenous Rspo1 in these cells were confirmed. ns, not significant. (D, E) Effect of *C*-mannosylation on intracellular trafficking. Cells were cultured with 50 μg/ml soluble heparin, stained with Hoechst 33258 (blue), anti–c-myc (green), and anti-KDEL (red; D) or anti-GRASP65 (red; E), and examined by fluorescence microscopy. Areas of overlapping stains are represented in yellow in the superimposed images. Bars, 10 μm. (F) Effect of *C*-mannosylation on Rspo1 secretion using a mutant Rspo1-overexpressing cell line. Cells were cultured with 50 μg/ml soluble heparin, and cell lysates and conditioned media were electrophoresed and

only DPY19L3 mediates *C*-mannosylation of Rspo1 at W^{156} and that no DPY19 member is a *C*-mannosyltransferase of Rspo1 at W^{153}.

DPY19L3-mediated *C*-mannosylation of Rspo1 at W^{156} regulates its secretion

Because *C*-mannosylation of Rspo1 is required for its secretion (Figure 3, A and F), we determined the effects of depleting DPY19L3 on Rspo1 secretion. We depleted DPY19L1, DPY19L3, or DPY19L4 by siRNA-mediated knockdown and measured levels of secreted Rspo1 (Figures 5B and 6A). Knockdown of DPY19L3, but not DPY19L1 or DPY19L4, decreased secreted Rspo1 levels and accumulated intracellular Rspo1 (Figure 6A). To exclude any off-target effects, we used another siRNA sequence against DPY19L3 and obtained similar results (Figure 6, B and C). These results indicate that DPY19L3-mediated *C*-mannosylation of Rspo1 at W^{156} is important for its secretion.

Finally, we assessed TOPFlash activity of Rspo1 derived from DPY19L3-depleted cells. Silencer green fluorescent protein (siGFP)–treated cells produce dimannosylated Rspo1 (at both W^{153} and W^{156}) and mono-*C*-mannosylated Rspo1 (only at W^{153}); siDPY19L3-treated cells produce mainly monomannosylated Rspo1 (only at W^{153}) and a trace amount of dimannosylated Rspo1 (at both W^{153} and W^{156}; Figure 5C). We purified these Rspo1s from each culture medium and used equal amounts of each protein for stimulation (Figure 6D, inset). The TOPFlash activity of 293T cells stimulated with Rspo1 produced by siDPY19L3-treated cells was not changed compared with that by siGFP-treated cells (Figure 6D). These results suggested that monomannosylated Rspo1 (only at W^{153}) has almost the same activity as dimannosylated Rspo1 (at both W^{153} and W^{156}). Figure 4C shows that monomannosylated Rspo1 (only at W^{156}) has increased activity compared with nonmannosylated Rspo1. The combined results (Figures 4C and 6D) suggest that the existence of *C*-mannosylation of Rspo1, at least either at W^{153} or W^{156}, is important for the enhancing activity of Wnt signaling.

DISCUSSION

In this study, we showed that human Rspo1 is *C*-mannosylated at W^{153} and W^{156} in the TSR1 (Figure 2) and that *C*-mannosylation of Rspo1 regulates its secretion and canonical Wnt/β-catenin signaling (Figure 3). Because all Rspo members have two conserved tryptophan residues in the TSR1 (Figure 1B), they are likely to undergo *C*-mannosylation, having similar functions between proteins. In previous reports, the two Fu domains of Rspos were sufficient and essential to enhance Wnt signaling (Kazanskaya *et al.*, 2004; Nam *et al.*, 2006; Kim *et al.*, 2008). In our study, however, we demonstrated the following three results about the effect of *C*-mannosylation of Rspo1 on Wnt signaling enhancing activity. 1) Rspo1/2WA, which lacks *C*-mannosylation due to alanine substitutions at W^{153} and W^{156}, had less activity than wild-type Rspo1 (Figure 3H); 2) the activity of mono-*C*-mannosylated Rspo1 at only W^{156}, which was produced by DPY19L3-expressing S2 cells, was increased compared with nonmannosylated Rspo1 (Figure 4C); and 3) the activity of mono-*C*-mannosylated Rspo1 at only W^{153}, which was produced by DPY19L3-depleted HT1080-Rspo1-MH cells, was not changed compared with wild-type Rspo1 (Figure 6D). These results suggested that not only two Fu domains, but also *C*-mannosylation of Rspo1, at least at either W^{153} or W^{156}, is important for Wnt signaling–enhancing activity. Because the *C*-mannosylation sites of Rspo1 reside in the TSR1, which is necessary for binding HSPG (Nam *et al.*, 2006; Carlson *et al.*, 2008), we measured the affinity of wild-type and the 2WA mutant Rspo1 to heparin–Sepharose beads. Their affinities were nearly the same (unpublished data). Thus the differences in Wnt signaling activity between *C*-mannosylated and non-*C*-mannosylated Rspo1 might be attributed to their three-dimensional structures, stability, or affinity to its receptors. Although further studies are required to determine the regulatory mechanism of Rspo1 activity by *C*-mannosylation, we conclude that *C*-mannosylation of Rspo1—a novel method of regulating Rspo1 function—is important in enhancing Wnt signaling.

A previous study demonstrated that *C. elegans* DPY19 is a *C*-mannosyltransferase of TSR1 peptide and suggested that human DPY19L1–L4 have *C*-mannosyltransferase activity (Buettner *et al.*, 2013). In our study, we provided the first experimental evidence that human DPY19L3 is a *C*-mannosyltransferase of Rspo1 at W^{156}, through gain- and loss-of-function experiments (Figures 4 and 5). These results indicate that DPY19 family members have substrate specificity and imply the existence of *C*-mannosyltransferase(s) other than the DPY19 family, because DPY19L1–L4 are not *C*-mannosyltransferases of Rspo1 at W^{153}. Initially, we believed that *C*-mannosylation of Rspo1 at both sites occurred sequentially because mono-*C*-mannosylated Rspo1 at W^{156} was not observed by LC-MS; however, DPY19L3 attaches one mannose residue to W^{156} but not W^{153} (Figure 4), suggesting that *C*-mannosylation of Rspo1 at these two sites is elicited by independent pathways. In vertebrate evolution, DPY19 split into DPY19L1, DPY19L3, and DPY19L4, and DPY19L1 diverged into DPY19L1 and DPY19L2 in mammals (Carson *et al.*, 2006; Buettner *et al.*, 2013). Human DPY19L1 is the closest homologue of *C. elegans* DPY19 (51% identity), followed by DPY19L2 (41%), DPY19L3 (36%), and DPY19L4 (33%; Buettner *et al.*, 2013). Thus DPY19L1 has been proposed to have *C*-mannosyltransferase activity in humans, but based on our results, all DPY19 proteins likely have such activity. Further analyses are needed to determine whether each DPY19 member is functional and has substrate specificity and identify the *C*-mannosyltransferase of Rspo1 at W^{153}.

In this study, we demonstrated that Rspo1 is *C*-mannosylated at W^{153} and W^{156} and that the functions are regulated by *C*-mannosylation. Further, we also provide evidence that human DPY19L3 is the

immunoblotted with anti–c-myc and anti–α-tubulin. Signal intensities of Rspo1 were quantified and normalized to α-tubulin expression using ImageJ software. The Rspo1/α-tubulin ratio (wt) was defined as 1.0. (G) Effect of *C*-mannosylation on the kinetics of Rspo1 secretion. Cells were cultured with 50 µg/ml soluble heparin, and conditioned media were collected at the indicated times, electrophoresed, and immunoblotted with anti–c-myc (top). Protein bands were quantified by using ImageJ software (bottom). The secreted amount of wild-type Rspo1 at 24 h was defined as 100%. (H) Effect of *C*-mannosylation on Rspo1-mediated enhancement of Wnt signaling. Recombinant Rspo1 and Rspo1/2WA were purified from each cell line, and the amounts of proteins were equalized by Western blot (inset). 293T cells were transfected with TOPFlash or FOPFlash in the presence of 10% Wnt3a-conditioned medium and treated with equal amounts of purified Rspo1. After 24 h, luciferase activities were measured and normalized to *Renilla* luciferase. Non–C-mannosylated Rspo1 slightly enhanced Wnt signaling activity. Data shown are means ± SD. *$p < 0.05$ compared with FOPFlash of vehicle control treatment. **$p < 0.05$ compared with TOPFlash of vehicle control treatment. ***$p < 0.05$ compared with TOPFlash of vehicle control and wild-type Rspo1 treatments.

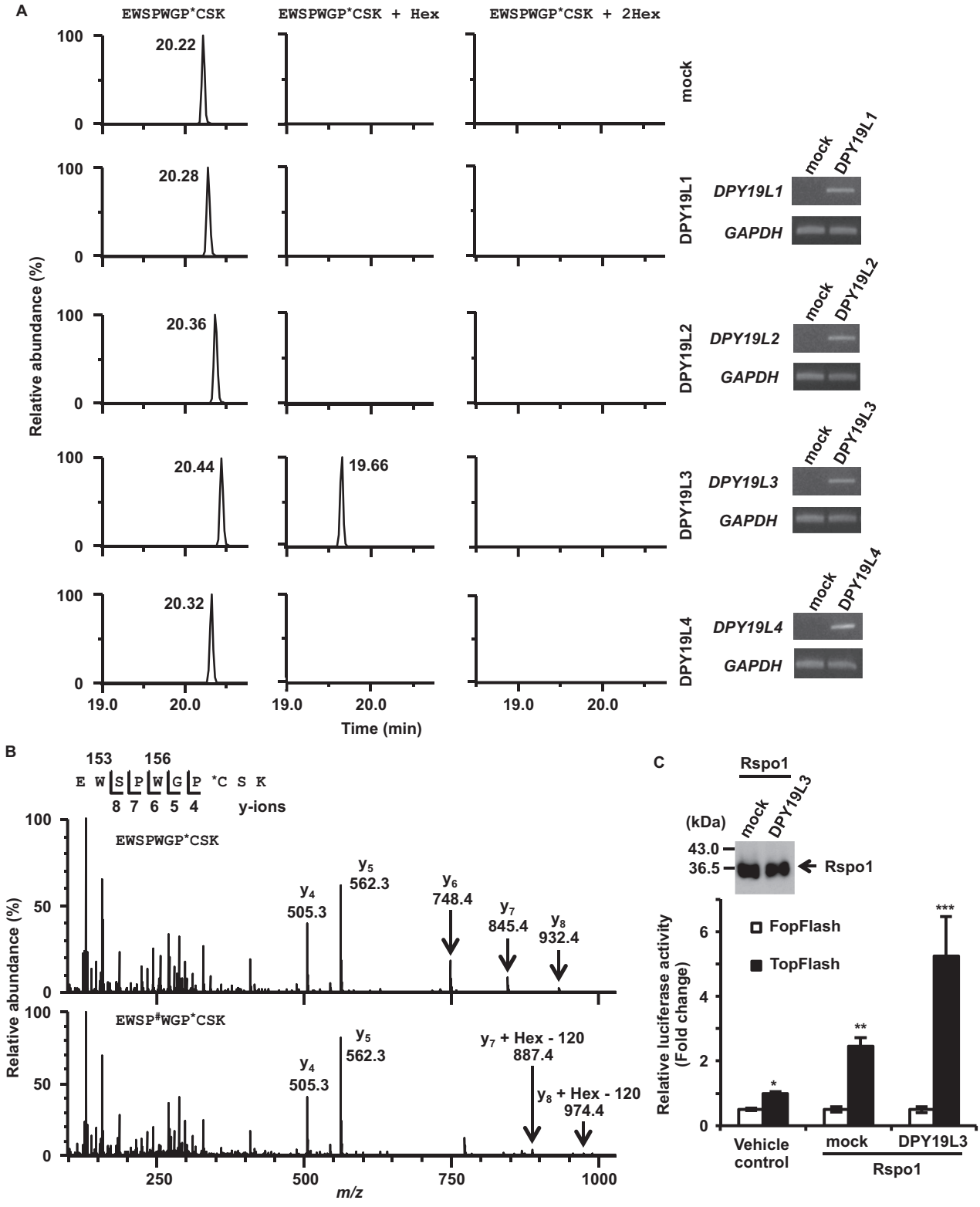

FIGURE 4: DPY19L3 is the *C*-mannosyltransferase of Rspo1 at W^{156}. (A, B) Identification of *C*-mannosyltransferase of Rspo1. Human DPY19L1-L4– or empty vector (mock)–expressing *Drosophila* S2 cells were transiently transfected with pMT-Rspo1-MH, and protein expression was induced by 200 μM $CuSO_4$ for 72 h. Rspo1-MH protein was purified by tandem affinity chromatography, heparin–Sepharose, and Ni-NTA agarose. The samples were digested with trypsin and Asp-N, and the resulting peptides were analyzed by LC-MS/MS. Monomannosylated peptide was observed only when the protein was produced in DPY19L3-expressing S2 cells (A). Unmannosylated and monomannosylated peptides derived from DPY19L3-expressing S2 cells were further analyzed by LC-MS/MS. Indicated *y* ions were detected, and signals resulting from the characteristic cross-ring cleavages were observed at the y_7 and y_8 ions in monomannosylated peptide (B). #W, *C*-mannosyltryptophan; *C, propionamide cysteine. (C) Effect of *C*-mannosylation of Rspo1 at W^{156} on

C-mannosyltransferase of Rspo1 at W^{156} and that DPY19L3-mediated *C*-mannosylation of Rspo1 at W^{156} governs its secretion. Although *C*-mannosylation of Rspo1 at W^{153} is also important to understanding Rspo1 function, we provided experimental findings that identify DPY19L3 as a *C*-mannosyltransferase in human cells, increasing our understanding of *C*-mannosylation.

MATERIALS AND METHODS

Cell culture

The HT1080 human fibrosarcoma and 293T human embryonic kidney cell lines were cultured in DMEM (Nissui, Tokyo, Japan) supplemented with 10% (vol/vol) fetal bovine serum, 100 U/ml penicillin G, 100 mg/l kanamycin, 600 mg/l L-glutamine, and 2.25 g/l $NaHCO_3$ at 37°C in a humidified incubator with 5% CO_2. The CHO-K1 Chinese hamster ovary and its subline Lec15.2 cells (Camp *et al.*, 1993) were cultured in Ham's F-12K (Sigma-Aldrich, St. Louis, MO) supplemented with 5% (vol/vol) fetal bovine serum (FBS), 100 U/ml penicillin G, 100 mg/l kanamycin, and 2.5 g/l $NaHCO_3$ at 37°C in a humidified incubator with 5% CO_2. The S2 *Drosophila melanogaster* embryo cell line was cultured in Schneider's *Drosophila* medium (Life Technologies, Carlsbad, CA) supplemented with 10% (vol/vol) heat-inactivated FBS, 100 U/ml penicillin G, and 100 mg/l kanamycin at 25°C.

Plasmid construction

Wild-type Rspo1-MH and Rspo1/N137Q-MH cDNAs, which were subcloned into pCI-neo vectors (Promega, Madison, WI), were constructed previously (Tsuchiya *et al.*, 2016). We substituted certain Trp residues in Rspo1 with Ala by PCR site-directed mutagenesis using the overlap extension technique. The sequences of primers for the mutagenesis were, for W153A, 5′-GTGAAATGAGCGAGGCGTCTCCGTGGGGGC-3′ (forward) and 5′-GCCCCCACGGAGACGCCTCGCTCATTTCAC-3′ (reverse); and for W156A, 5′-GTCTCCGGCGGGGCCCTGC-3′ (forward) and 5′-GCAGGGCCCCGCCGGAGAC-3′ (reverse). The resulting cDNAs were cloned into the *Xho*I/*Not*I restriction sites of pCI-neo for mammalian cell expression.

For expression in S2 cells, Rspo1-myc cDNA was amplified from pCI-neo-Rspo1-MH and subcloned into the *Bgl*II/*Mlu*I restriction sites of pMT-PURO (RIKEN BioResource Center, Tsukuba, Japan; Iwaki and Castellino, 2008), resulting in expression of Rspo1-MH protein.

Human DPY19L1, DPY19L3, and DPY19L4 cDNA were amplified from an HT1080 cell cDNA library, and human DPY19L2 cDNA was amplified from a PC3 cell cDNA library. Each cDNA was conjugated with a C-terminal myc tag by PCR and cloned into the *Eco*RI/*Mlu*I (DPY19L1 and DPY19L2) or *Not*I/*Mlu*I (DPY19L3 and DPY19L4) restriction sites of pIZ/V5-his (Life Technologies).

Generation of Rspo1-overexpressing cell lines

Permanent cell lines that expressed wild-type or mutant Rspo1-MH were established by transfecting the vectors into HT1080 cells, followed by selection with 400 µg/ml G418 (Roche Applied Sciences, Basel, Switzerland). The clones that expressed high levels of wild-type Rspo1 and Rspo1 (W153A and W156A) were designated HT1080-Rspo1-MH (Tsuchiya *et al.*, 2016) and HT1080-Rspo1/2WA-MH cells, respectively. The cells that were transfected with pCI-neo were termed HT1080-neo.

Western blot

We performed Western blot using a slightly modified version of a previously described method (Niwa *et al.*, 2012; Yasukagawa *et al.*, 2012; Goto *et al.*, 2014a,b; Komai *et al.*, 2015). Cells were cultured and lysed in lysis buffer (50 mM Tris-HCl, pH 7.5, 150 mM NaCl, 0.1% [wt/vol] SDS, 1% [vol/vol] Triton X-100, 1% [wt/vol] sodium deoxycholate, and 1 mM phenylmethylsulfonyl fluoride) at 4°C with sonication. The lysates were centrifuged at 14,000 rpm for 10 min, and the amount of protein in each lysate was measured by Coomassie Brilliant Blue (CBB) G-250 staining (Bio-Rad Laboratories, Hercules, CA). Loading buffer (350 mM Tris-HCl, pH 6.8, 30% [wt/vol] glycerol, 0.012% [wt/vol] bromophenol blue, 6% [wt/vol] SDS, and 30% [vol/vol] 2-mercaptoethanol) was added to each lysate, which was subsequently boiled for 3 min and electrophoresed on SDS–polyacrylamide gels. Proteins were transferred to polyvinylidene fluoride membranes and immunoblotted with anti–c-myc (C3956; Sigma-Aldrich) or anti–α-tubulin (T5168; Sigma-Aldrich). Signals were detected with enhanced chemiluminescence reagent (Immobilon Western Chemiluminescent HRP Substrate; Millipore, Billerica, MA) on an ImageQuant LAS4000mini (GE Healthcare, Little Chalfont, United Kingdom).

Detection of secreted Rspo1

Cells were washed with phosphate-buffered saline (PBS) twice and cultured in serum-free DMEM for 24 h with or without 50 µg/ml soluble heparin (Sigma-Aldrich). The conditioned media were collected, and cell lysates were prepared as described. Loading buffer was added to the conditioned media and cell lysates, which were boiled for 3 min. Then the proteins were separated by SDS–PAGE and analyzed by immunoblot with anti–c-myc and anti–α-tubulin. Quantitation of protein bands was performed using ImageJ software (National Institutes of Health, Bethesda, MD).

Purification of recombinant wild-type Rspo1 for LC-MS

To purify recombinant wild-type Rspo1, we used a slightly modified version of a previously described method (Niwa *et al.*, 2012; Goto *et al.*, 2014a,b). Cells were washed with PBS twice and cultured in serum-free DMEM for 24 h with 50 µg/ml soluble heparin. After 24 h, the conditioned medium was collected, precipitated with ammonium sulfate, and resuspended in PBS. After being dialyzed in PBS, Ni-NTA agarose (Qiagen, Hilden, Germany) was added to the samples, and the mixture was incubated for 2 h at 4°C. The Ni-NTA agarose was washed three times with buffer A (900 mM NaCl, 2.7 mM KCl, 10 mM Na_2HPO_4, 1.8 mM KH_2PO_4, and 20 mM imidazole), and Ni-NTA agarose-bound Rspo1 was eluted with 500 mM imidazole. The eluates were electrophoresed on an SDS–polyacrylamide gel, and the protein bands were visualized by CBB staining.

Wnt signaling–enhancing activity. Recombinant Rspo1 proteins produced by mock- or DPY19L3-transfected S2 cells were purified, and the amounts of proteins were equalized by Western blot (inset). 293T cells were transfected with TOPFlash or FOPFlash in the presence of 10% Wnt3a-conditioned medium and treated with equal amounts of purified Rspo1 proteins. After 24 h, luciferase activities were measured and normalized to *Renilla* luciferase. *C*-mannosylated Rspo1 at W^{156} (produced by DPY19L3-expressing S2 cells) had increased activity compared with non–*C*-mannosylated Rspo1 (produced by mock-transfected S2 cells). Data shown are means ± SD. *$p < 0.05$ compared with FOPFlash of vehicle control treatment. **$p < 0.05$ compared with TOPFlash of vehicle control treatment. ***$p < 0.05$ compared with TOPFlash of vehicle control and mock-produced Rspo1 treatments.

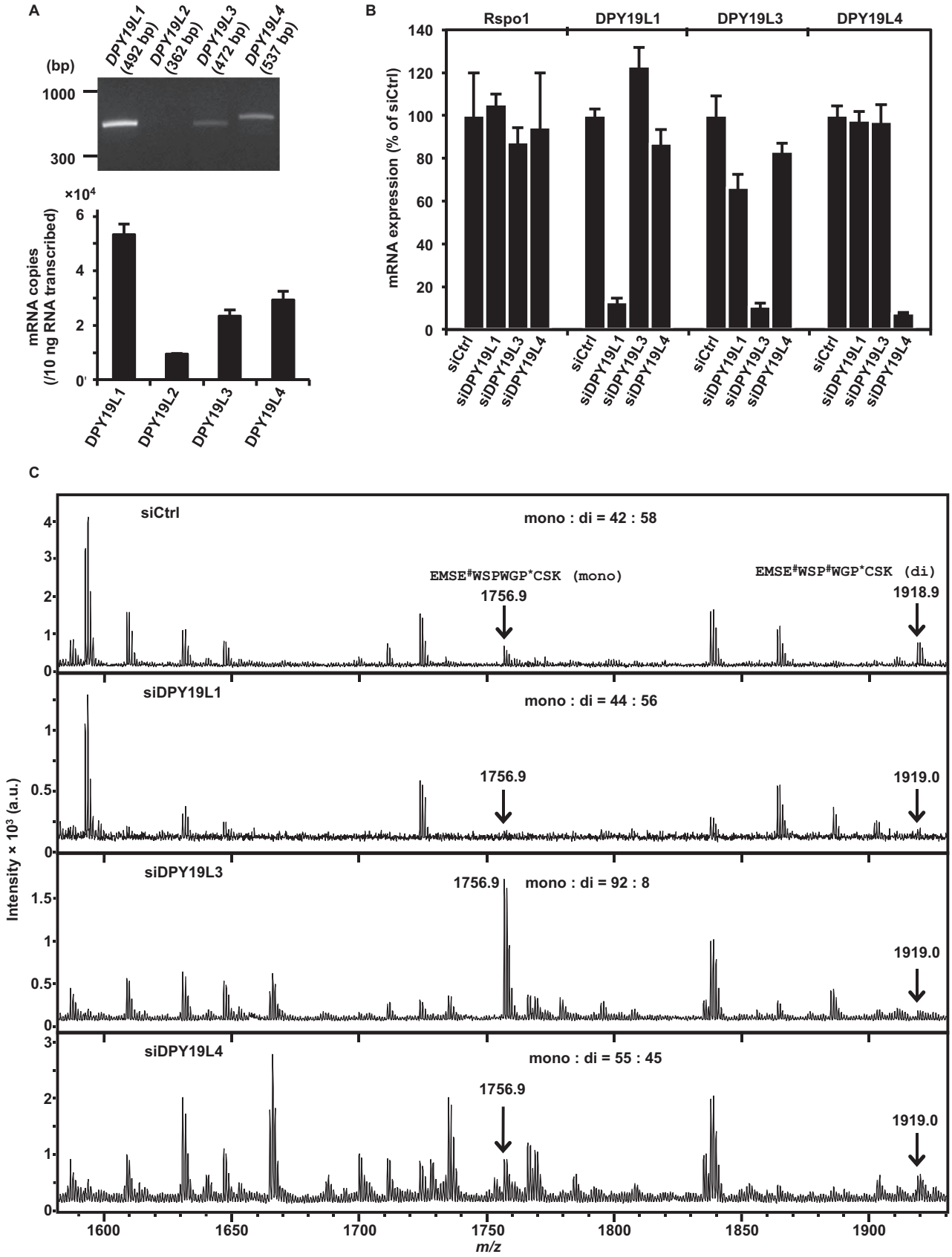

FIGURE 5: DPY19L3 is the *C*-mannosyltransferase of Rspo1 at W^{156} in human cells. (A) Expression of DPY19 members in HT1080-Rspo1-MH cells. Total RNA was isolated from HT1080-Rspo1-MH cells, and semiquantitative (top) and quantitative (bottom) RT-PCR were performed. Absolute copy number of mRNA transcript/10 ng of total RNA was calculated by quantitative RT-PCR. DPY19L2 expression was lower than the others. (B) Knockdown of DPY19L1,

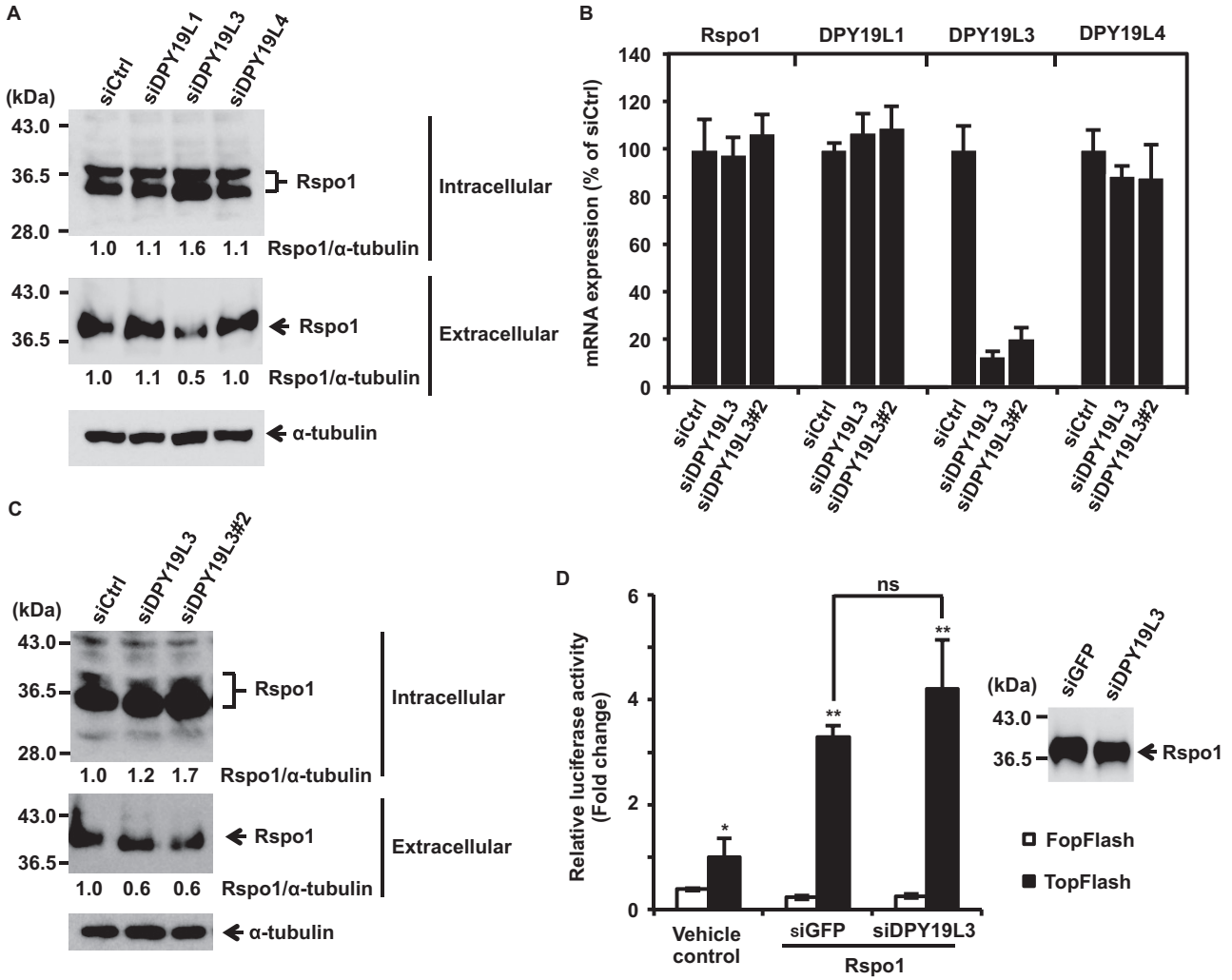

FIGURE 6: DPY19L3-mediated *C*-mannosylation of Rspo1 at W^{156} regulates its secretion. (A) Effect of knockdown of DPY19L1, DPY19L3, or DPY19L4 on Rspo1 secretion. HT1080-Rspo1-MH cells were treated with the indicated siRNAs and cultured in serum-free medium with 50 μg/ml soluble heparin, and cell lysates and conditioned media were electrophoresed and immunoblotted with anti–c-myc and anti–α-tubulin. Signal intensities of Rspo1 were quantified and normalized to α-tubulin expression using ImageJ software. The Rspo1/α-tubulin ratio (siCtrl) was defined as 1.0. (B, C) Effect of knockdown of DPY19L3 on Rspo1 secretion. HT1080-Rspo1-MH cells were treated with the indicated siRNAs. Total RNA was isolated from each cell line, and quantitative RT-PCR was performed (B). Each cell line was cultured in serum-free medium with 50 μg/ml soluble heparin, and cell lysates and conditioned media were electrophoresed and immunoblotted with anti–c-myc and anti–α-tubulin (C). Signal intensities of Rspo1 were quantified and normalized to α-tubulin expression using ImageJ software. The Rspo1/α-tubulin ratio (siCtrl) was defined as 1.0. (D) Effect of *C*-mannosylation of Rspo1 at W^{153} on Wnt signaling enhancing activity. HT1080-Rspo1-MH cells were treated with siGFP or siDPY19L3, and conditioned medium from each cell was collected. Rspo1 proteins were purified from the conditioned medium of siGFP- or siDPY19L3-treated cells, and the amounts of proteins were equalized by Western blot (inset). 293T cells were transfected with TOPFlash or FOPFlash in the presence of 10% Wnt3a-conditioned medium and treated with equal amounts of purified Rspo1 proteins. After 24 h, luciferase activities were measured and normalized to *Renilla* luciferase. W^{153}-*C*-mannosylated Rspo1 (produced by siDPY19L3-treated cells) had almost same activity as wild-type Rspo1 (produced by siGFP-treated cells). Data shown are means ± SD. *$p < 0.05$ compared with FOPFlash of vehicle control treatment. **$p < 0.05$ compared with TOPFlash of vehicle control treatment. ns, not significant.

DPY19L3, and DPY19L4. Total RNA was isolated from each cell line, and quantitative RT-PCR was performed. Significant knockdown efficiency was observed for each siRNA against its target gene. (C) DPY19L3 is the *C*-mannosyltransferase of Rspo1 at W^{156} in human cells. HT1080-Rspo1-MH cells were treated with the indicated siRNAs, and conditioned media were collected. Recombinant Rspo1 was purified with Ni-NTA agarose, and the samples were digested with trypsin and Asp-N. The resulting peptides were analyzed by MALDI-TOF MS. siDPY19L3 changed the ratio of two peptides compared with siCtrl: the signal intensity from the dimannosylated peptide at W^{153} and W^{156} ($m/z = 1919.0$) declined, although that of the monomannosylated peptide at W^{153} ($m/z = 1756.9$) increased. #W, *C*-mannosyltryptophan; *C, propionamide cysteine. The ratio monomannosylated/dimannosylated Rspo1 was calculated from each peak area.

LC-MS

To identify the *C*-mannosylation sites, we used the ultrasensitive Q-Exactive nanoLC-MS/MS system (Michalski *et al.*, 2011). Purified Rspo1 samples were subjected to SDS–PAGE. After CBB staining, the visible band was excised and destained. In-gel digestion was performed using endoproteinase Asp-N (sequencing grade; Roche) and then trypsin (TPCK-treated; Worthington Biochemical, Worthington, OH). The digestion mixture was separated on a nanoflow LC (Easy nLC; Thermo Fisher Scientific, Waltham, MA) using a nano–electrospray ionization spray column (NTCC analytical column, C18, ϕ75 μm × 100 mm, 3 μm; Nikkyo Technos, Tokyo, Japan) with a linear gradient of 0–35% buffer B (100% acetonitrile and 0.1% formic acid) at a flow rate of 300 nl/min over 10 min, coupled on-line to a Q-Exactive mass spectrometer (Thermo Fisher Scientific) equipped with a nanospray ion source. MS and MS/MS data were acquired using the data-dependent top5 method. The resulting MS/MS data were searched against an in-house database, including the Rspo1 sequence, using MASCOT (Matrix Science, Boston, MA) with variable modifications: Gln → pyro-Glu (N-term Q), Oxidation (M), Propionamide (C), and Hex (W).

Transient transfection for CHO-K1 and Lec15.2 cells

CHO-K1 and Lec15.2 cells were transiently transfected with pCI-neo-Rspo1/N137Q-MH vector (Tsuchiya *et al.*, 2016) using Lipofectamine LTX reagent (Invitrogen, Carlsbad, CA). After 6 h of transfection, cells were washed with PBS and further cultured in serum-free medium with 50 μg/ml soluble heparin for 18 h. The conditioned media and cell lysates were collected and prepared as described. Loading buffer was added to the conditioned media and cell lysates, which were boiled for 3 min. Then the proteins were separated by SDS–PAGE and analyzed by immunoblot with anti–c-myc and anti–α-tubulin.

Quantitative RT-PCR

Total RNA was extracted from cultured cells with TRIzol (Invitrogen) per the manufacturer's protocol, and solutions that contained 2 μg of total RNA were set aside for reverse transcription using the High-Capacity cDNA Reverse-Transcription Kit (Applied Biosystems, Waltham, MA). KOD SYBR qPCR Mix (TOYOBO, Osaka, Japan) was used for the quantitative RT-PCR, which was performed on an ABI 7500 Real-Time PCR System (Applied Biosystems).

The sequences of the primers for quantitative RT-PCR and their annealing temperatures were as follows: Rspo1, 5′-CTCTGCTCTGAAGTCAACGG-3′ (forward) and 5′-CACTCGCTCATTTCACATTG-3′ (reverse), 63°C; DPY19L1, 5′-GGCATCACTGATCTGCTCAA-3′ (forward) and 5′-AAGGGAGTTTTCCCAGCATT-3′ (reverse), 60°C; DPY19L2, 5′-GAAAAGGCTTGGAGCTAGAGGTG-3′ (forward) and 5′-GATGAGAGGTGAGAGAAATGACGA-3′ (reverse), 60°C; DPY19L3, 5′-CCCTGAAATATGGGAGTTACTTCTG-3′ (forward) and 5′-CACAGCCTTTCTTGGAGTGTTAG-3′ (reverse), 60°C; DPY19L4, 5′-GCCAAATTGCTGCACTTACA-3′ (forward) and 5′-GCAGGGATTCTTGACAGAGG-3′ (reverse), 60°C; and β-actin, 5′-CTTCTACAATGAGCTGCGTG-3′ (forward) and 5′-TCATGAGGTAGTCAGTCAGG-3′ (reverse), 58°C.

To determine the absolute copy number of mRNAs, each cDNA was amplified and subcloned into pGEM-T Easy (Promega). The plasmids were linearized with *Nae*I, electrophoresed on agarose gels, and purified using the GENECLEAN II Kit (MP Biomedicals, Santa Ana, CA). The samples were quantified by ultraviolet (UV) absorbance at 260 nm on a BioPhotometer plus (Eppendorf, Hamburg, Germany) and serially diluted 10-fold, yielding a range of 10^3–10^7 copies. These dilutions and reverse-transcribed cDNA were subjected to quantitative RT-PCR, and absolute copy numbers of mRNAs per 10 ng of total RNA were calculated.

Semiquantitative RT-PCR

Semiquantitative RT-PCR was performed using a slightly modified version of previously described methods (Niwa *et al.*, 2012; Yasukagawa *et al.*, 2012; Goto *et al.*, 2014b; Komai *et al.*, 2015). The sequences of the primers for semiquantitative RT-PCR, numbers of cycles, and annealing temperatures were as follows: Rspo1-MH, 5′-CTCTGCTCTGAAGTCAACGG-3′ (forward) and 5′-GTGATGGTGATGATGCAGATCCTCTTCTGAGATGAG-3′ (reverse), 25 cycles, 63°C; DPY19L1, 5′-GGCATCACTGATCTGCTCAA-3′ (forward) and 5′-AAGGGAGTTTTCCCAGCATT-3′ (reverse), 25 cycles, 60°C; DPY19L2, 5′-ATGAGAAAACAAGGAGTAAGCTCAAAGCGG-3′ (forward) and 5′-CAATGTAAAATTGCCACAAAGACAG-3′ (reverse), 25 cycles, 60°C; DPY19L3, 5′-AGTTCTGGCCAGGAATGATG-3′ (forward) and 5′-ACGTAGGGAGGCAGGTTTCT-3′ (reverse), 25 cycles, 60°C; DPY19L4, 5′-GCCAAATTGCTGCACTTACA-3′ (forward) and 5′-GCAGGGATTCTTGACAGAGG-3′ (reverse), 25 cycles, 60°C; β-actin, 5′-CTTCTACAATGAGCTGCGTG-3′ (forward) and 5′-TCATGAGGTAGTCAGTCAGG-3′ (reverse), 20 cycles, 58°C; and glyceraldehyde-3-phosphate dehydrogenase 2, 5′-GTCCTATGATGAAATTAAGGCCAAG-3′ (forward) and 5′-GTCGTACCAAGAGATCAGCTTCAC-3′ (reverse), 25 cycles, 60°C.

PCR products were electrophoresed on agarose gels, stained with ethidium bromide, and visualized on a UV illuminator.

Immunofluorescence

To observe intracellular trafficking, we used a slightly modified version of previously described methods (Niwa *et al.*, 2012; Yasukagawa *et al.*, 2012). Cells were grown in the presence of 50 μg/ml soluble heparin on coverslips, washed with PBS, fixed in 4% paraformaldehyde for 10 min, and permeabilized with 0.1% Triton X-100 for 10 min. After a blocking step with 3% bovine serum albumin, the cells were incubated with mouse monoclonal anti–c-myc (sc-40; Santa Cruz Biotechnology, Santa Cruz, CA) or rabbit polyclonal anti–c-myc (C3956; Sigma-Aldrich) for 1 h. Alexa Fluor 488–conjugated anti-mouse immunoglobulin G (IgG; Molecular Probes, Waltham, MA) and Alexa Fluor 488–conjugated anti-rabbit IgG (Molecular Probes) were used as the secondary antibodies.

To detect the Golgi apparatus and ER, the cells were incubated with rabbit polyclonal anti-GRASP65 (sc-30093; Santa Cruz Biotechnology) and mouse monoclonal anti-KDEL (ADI-SPA-827; Enzo Life Sciences, Farmingdale, NY), respectively. Alexa Fluor 568–conjugated anti-rabbit IgG (Molecular Probes) and Alexa Fluor 568–conjugated anti-mouse IgG (Molecular Probes) were used as the secondary antibodies. After being washed two additional times, the cells were incubated with 2 μg/ml Hoechst 33258 (Polysciences, Warrington, PA) for 10 min to stain the nuclei. The cells were washed with PBS and examined under a fluorescence microscope (EVOS FL Cell Imaging System; Life Technologies).

Purification of recombinant Rspo1 for luciferase assay

Cells were washed twice with PBS and cultured in serum-free DMEM for 24 h with 1% (vol/vol) Heparin Sepharose 6 Fast Flow (GE Healthcare). After 24 h, heparin–Sepharose beads were collected, washed twice with PBS, and eluted with 900 mM NaCl (buffer A). Ni-NTA agarose was added, and the mixture was incubated for 2 h at 4°C and eluted with 500 mM imidazole. Eluates were concentrated and buffer-exchanged with PBS on a VIVASPIN 500 (Sartorius, Göttingen, Germany). Purified Rspo1 was electrophoresed and immunoblotted with anti–c-myc, and each sample was diluted to equalize protein

content. Equal amounts of purified Rspo1 were used for the luciferase assay, as described next.

Luciferase reporter assay

293T cells were plated into 24-well plates. After 24 h, the cells were transiently transfected with 400 ng of canonical Wnt signaling reporter Super 8×TopFlash (Addgene plasmid 12456) or mutant reporter Super 8×FopFlash (Addgene plasmid 12457; Veeman *et al.*, 2003) and 20 ng of phRL-TK vector (Promega) in the presence of 10% (vol/vol) Wnt3a-conditioned medium (Carmon *et al.*, 2012) from L-Wnt3a cells (ATCC CRL-2647) as described (Willert *et al.*, 2003). Then the cells were treated with equal amounts of Rspo1 proteins. After 24 h, the cells were lysed, and luciferase activities were measured. TOPFlash and FOPFlash activities were normalized to those of *Renilla* luciferase.

Protein expression in S2 cells

S2 cells were transfected with pIZ-DPY19L1, pIZ-DPY19L2, pIZ-DPY19L3, pIZ-DPY19L4, or pIZ using FuGENE HD Transfection Reagent (Promega) and selected with 150 µg/ml Zeocin (Life Technologies) for 2 wk. Then each line was plated into six-well plates and transiently transfected with pMT-Rspo1-MH. After 6 h, the cells were washed and cultured in serum-free medium with 200 µM $CuSO_4$ to induce Rspo1 expression. After 72 h of induction, cultured media were collected and applied to heparin–Sepharose beads. After 90 min of agitation, heparin–Sepharose–bound proteins were eluted with 900 mM NaCl (buffer A), and the eluates were further purified with Ni-NTA agarose. Ni-NTA agarose–bound Rspo1 was eluted with 500 mM imidazole. For LC-MS analysis, the resulting samples were electrophoresed on an SDS–polyacrylamide gel. The protein bands were visualized by CBB, and purified samples were analyzed by LC-MS as described. For the luciferase assay, purified Rspo1 was electrophoresed and immunoblotted with anti–c-myc, and each sample was diluted to equalize protein content. Equal amounts of purified Rspo1 were used for the luciferase assay, as described.

Knockdown of DPY19 members

Cells were transfected with 20 nM siRNA using Lipofectamine RNAiMAX (Invitrogen). The knockdown efficiencies of the siRNAs against each target gene were measured by quantitative RT-PCR. The sequences of the siRNAs were as follows: siCtrl, CGUACGCGGAUACUUCGAdTdT; siDPY19L1, GCACUUCGGCCCAUUGUGAdTdT; siDPY19L3, GGAUAUGUAUAAUGCGAUAdTdT; siDPY19L3#2, GAAACUGCCUACAACUUAAdTdT; and siDPY19L4, GGUGUGUACUCUGACAAUAdTdT. siGFP siRNA (AM4626) was purchased from Applied Biosystems.

Purification of recombinant Rspo1 from DPY19-deficient cells

The DPY19-deficient cells were cultured in serum-free DMEM for 24 h with 50 µg/ml heparin, and culture medium samples were collected. The samples were concentrated on Amicon Ultra-15 Centrifugal Filter Devices (Millipore Corporation), and 8 M urea was added. Ni-NTA agarose was added to the samples, and the mixture was incubated for 2 h at 4°C. The Ni-NTA agarose was washed three times with buffer A, and Ni-NTA agarose–bound Rspo1 was eluted with 500 mM imidazole. The eluates were electrophoresed on an SDS–polyacrylamide gel, and the protein bands were visualized by CBB staining. Purified Rspo1 was analyzed by MALDI-TOF MS.

MALDI-TOF MS

Purified recombinant Rspo1 was separated on SDS–polyacrylamide gels. After CBB staining, the bands were excised, treated with 0.05 µg of sequencing-grade modified trypsin (Promega) and endoproteinase Asp-N (Roche Diagnostics) at 37°C for 12 h in 0.1 M Tris-HCl, pH 8.0, and reduced by propionamidation. The digests were desalted using C18µ ZipTips (Millipore) and analyzed by MALDI-TOF MS on an ultrafleXtreme TOF/TOF MS (Bruker Daltonics, Billerica, MA) in reflector mode using α-cyano-4-hydroxycinnamic acid as a matrix. The selected peaks were analyzed by MS/MS in LIFT mode.

Statistical analysis

Statistical analyses were performed using a two-tailed Student's *t*-test. The results are expressed as means ± SD. In the figures, significant *p* values are shown as $p < 0.05$ (*,**,***).

ACKNOWLEDGMENTS

We thank R. T. Moon for providing Super 8×TopFlash and Super 8×FopFlash. This work was supported in part by Grants-in-Aid for Scientific Research (B) (24310167) and a Japan Society for the Promotion of Science Fellowship (254256). Y.N. is a Research Fellow of the Japan Society for the Promotion of Science.

REFERENCES

Boldface names denote co–first authors.

Anastas JN, Moon RT (2013). WNT signalling pathways as therapeutic targets in cancer. Nat Rev Cancer 13, 11–26.

Buettner FF, Ashikov A, Tiemann B, Lehle L, Bakker H (2013). *C. elegans* DPY-19 is a *C*-mannosyltransferase glycosylating thrombospondin repeats. Mol Cell 50, 295–302.

Camp LA, Chauhan P, Farrar JD, Lehrman MA (1993). Defective mannosylation of glycosylphosphatidylinositol in Lec35 Chinese hamster ovary cells. J Biol Chem 268, 6721–6728.

Carlson CB, Lawler J, Mosher DF (2008). Structures of thrombospondins. Cell Mol Life Sci 65, 672–686.

Carmon KS, Gong X, Yi J, Thomas A, Liu Q (2014). RSPO-LGR4 functions via IQGAP1 to potentiate Wnt signaling. Proc Natl Acad Sci USA 111, E1221–E1229.

Carmon KS, Lin Q, Gong X, Thomas A, Liu Q (2012). LGR5 interacts and cointernalizes with Wnt receptors to modulate Wnt/β-catenin signaling. Mol Cell Biol 32, 2054–2064.

Carson AR, Cheung J, Scherer SW (2006). Duplication and relocation of the functional *DPY19L2* gene within low copy repeats. BMC Genomics 7, 45.

Chen PH, Chen X, Lin Z, Fang D, He X (2013). The structural basis of R-spondin recognition by LGR5 and RNF43. Genes Dev 27, 1345–1350.

de Lau W, Barker N, Low TY, Koo BK, Li VS, Teunissen H, Kujala P, Haegebarth A, Peters PJ, van de Wetering M, *et al.* (2011). Lgr5 homologues associate with Wnt receptors and mediate R-spondin signalling. Nature 476, 293–297.

Dezső Z, Nikolsky Y, Sviridov E, Shi W, Serebriyskaya T, Dosymbekov D, Bugrim A, Rakhmatulin E, Brennan RJ, Guryanov A, *et al.* (2008). A comprehensive functional analysis of tissue specificity of human gene expression. BMC Biol 6, 49.

Doucey MA, Hess D, Cacan R, Hofsteenge J (1998). Protein *C*-mannosylation is enzyme-catalysed and uses dolichyl-phosphate-mannose as a precursor. Mol Biol Cell 9, 291–300.

Glinka A, Dolde C, Kirsch N, Huang YL, Kazanskaya O, Ingelfinger D, Boutros M, Cruciat CM, Niehrs C (2011). LGR4 and LGR5 are R-spondin receptors mediating Wnt/β-catenin and Wnt/PCP signalling. EMBO Rep 12, 1055–1061.

Gong X, Yi J, Carmon KS, Crumbley CA, Xiong W, Thomas A, Fan X, Guo S, An Z, Chang JT, Liu QJ (2015). Aberrant RSPO3-LGR4 signaling in Keap1-deficient lung adenocarcinomas promotes tumor aggressiveness. Oncogene 34, 4692–4701.

Goto Y, Niwa Y, Suzuki T, Dohmae N, Umezawa K, Simizu S (2014a). *C*-mannosylation of human hyaluronidase 1: possible roles for secretion and enzymatic activity. Int J Oncol 45, 344–350.

Goto Y, Niwa Y, Suzuki T, Uematsu S, Dohmae N, Simizu S (2014b). *N*-glycosylation is required for secretion and enzymatic activity of human hyaluronidase1. FEBS Open Bio 4, 554–559.

Hamming OJ, Kang L, Svensson A, Karlsen JL, Rahbek-Nielsen H, Paludan SR, Hjorth SA, Bondensgaard K, Hartmann R (2012). Crystal structure of interleukin-21 receptor (IL-21R) bound to IL-21 reveals that sugar chain interacting with WSXWS motif is integral part of IL-21R. J Biol Chem 287, 9454–9460.

Hao HX, Xie Y, Zhang Y, Charlat O, Oster E, Avello M, Lei H, Mickanin C, Liu D, Ruffner H, *et al*. (2012). ZNRF3 promotes Wnt receptor turnover in an R-spondin-sensitive manner. Nature 485, 195–200.

Harbuz R, Zouari R, Pierre V, Ben Khelifa M, Kharouf M, Coutton C, Merdassi G, Abada F, Escoffier J, Nikas Y, *et al*. (2011). A recurrent deletion of *DPY19L2* causes infertility in man by blocking sperm head elongation and acrosome formation. Am J Hum Genet 88, 351–361.

Hofsteenge J, Huwiler KG, Macek B, Hess D, Lawler J, Mosher DF, Peter-Katalinic J (2001). *C*-mannosylation and *O*-fucosylation of the thrombospondin type 1 module. J Biol Chem 276, 6485–6498.

Hofsteenge J, Müller DR, de Beer T, Löffler A, Richter WJ, Vliegenthart JF (1994). New type of linkage between a carbohydrate and a protein: *C*-glycosylation of a specific tryptophan residue in human RNase U_s. Biochemistry 33, 13524–13530.

Ihara Y, Manabe S, Ikezaki M, Inai Y, Matsui IS, Ohta Y, Muroi E, Ito Y (2010). *C*-Mannosylated peptides derived from the thrombospondin type 1 repeat interact with Hsc70 to modulate its signaling in RAW264.7 cells. Glycobiology 20, 1298–1310.

Ilmer M, Boiles AR, Regel I, Yokoi K, Michalski CW, Wistuba II, Rodriguez J, Alt E, Vykoukal J (2015). RSPO2 enhances canonical Wnt signaling to confer stemness-associated traits to susceptible pancreatic cancer cells. Cancer Res 75, 1883–1896.

Iwaki T, Castellino FJ (2008). A single plasmid transfection that offers a significant advantage associated with puromycin selection in *Drosophila* Schneider S2 cells expressing heterologous proteins. Cytotechnology 57, 45–49.

Julenius K (2007). NetCGlyc 1.0: prediction of mammalian C-mannosylation sites. Glycobiology 17, 868–876.

Kamata T, Katsube K, Michikawa M, Yamada M, Takada S, Mizusawa H (2004). *R-spondin*, a novel gene with thrombospondin type 1 domain, was expressed in the dorsal neural tube and affected in *Wnt*s mutants. Biochim Biophys Acta 1676, 51–62.

Kazanskaya O, Glinka A, del Barco Barrantes I, Stannek P, Niehrs C, Wu W (2004). R-Spondin2 is a secreted activator of Wnt/β-catenin signaling and is required for *Xenopus* myogenesis. Dev Cell 7, 525–534.

Kim KA, Kakitani M, Zhao J, Oshima T, Tang T, Binnerts M, Liu Y, Boyle B, Park E, Emtage P, *et al*. (2005). Mitogenic influence of human R-spondin1 on the intestinal epithelium. Science 309, 1256–1259.

Kim KA, Wagle M, Tran K, Zhan X, Dixon MA, Liu S, Gros D, Korver W, Yonkovich S, Tomasevic N, *et al*. (2008). R-Spondin family members regulate the Wnt pathway by a common mechanism. Mol Biol Cell 19, 2588–2596.

Kim KA, Zhao J, Andarmani S, Kakitani M, Oshima T, Binnerts ME, Abo A, Tomizuka K, Funk WD (2006). R-Spondin proteins: a novel link to β-catenin activation. Cell Cycle 5, 23–26.

Komai K, Niwa Y, Sasazawa Y, Simizu S (2015). Pirin regulates epithelial to mesenchymal transition independently of Bcl3-Slug signaling. FEBS Lett 589, 738–743.

Koscinski I, Elinati E, Fossard C, Redin C, Muller J, Velez de la Calle J, Schmitt F, Ben Khelifa M, Ray P, Kilani Z, *et al*. (2011). *DPY19L2* deletion as a major cause of globozoospermia. Am J Hum Genet 88, 344–350.

Krieg J, Gläsner W, Vicentini A, Doucey MA, Löffler A, Hess D, Hofsteenge J (1997). *C*-Mannosylation of human RNase 2 is an intracellular process performed by a variety of cultured cells. J Biol Chem 272, 26687–26692.

Krieg J, Hartmann S, Vicentini A, Gläsner W, Hess D, Hofsteenge J (1998). Recognition signal for C-mannosylation of Trp-7 in RNase 2 consists of sequence Trp-x-x-Trp. Mol Biol Cell 9, 301–309.

Lehrman MA, Zeng Y (1989). Pleiotropic resistance to glycoprotein processing inhibitors in Chinese hamster ovary cells. The role of a novel mutation in the asparagine-linked glycosylation pathway. J Biol Chem 264, 1584–1593.

Michalski A, Damoc E, Hauschild JP, Lange O, Wieghaus A, Makarov A, Nagaraj N, Cox J, Mann M, Horning S (2011). Mass spectrometry-based proteomics using Q Exactive, a high-performance benchtop quadrupole Orbitrap mass spectrometer. Mol Cell Proteomics 10, M111.011015.

Nam JS, Turcotte TJ, Smith PF, Choi S, Yoon JK (2006). Mouse cristin/R-spondin family proteins are novel ligands for the Frizzled 8 and LRP6 receptors and activate β-catenin-dependent gene expression. J Biol Chem 281, 13247–13257.

Niehrs C (2012). The complex world of WNT receptor signalling. Nat Rev Mol Cell Biol 13, 767–779.

Niwa Y, Suzuki T, Dohmae N, Umezawa K, Simizu S (2012). Determination of cathepsin V activity and intracellular trafficking by N-glycosylation. FEBS Lett 586, 3601–3607.

Parma P, Radi O, Vidal V, Chaboissier MC, Dellambra E, Valentini S, Guerra L, Schedl A, Camerino G (2006). R-spondin1 is essential in sex determination, skin differentiation and malignancy. Nat Genet 38, 1304–1309.

Schuijers J, Clevers H (2012). Adult mammalian stem cells: the role of Wnt, Lgr5 and R-spondins. EMBO J 31, 2685–2696.

Shinmura K, Kahyo T, Kato H, Igarashi H, Matsuura S, Nakamura S, Kurachi K, Nakamura T, Ogawa H, Funai K, *et al*. (2014). RSPO fusion transcripts in colorectal cancer in Japanese population. Mol Biol Rep 41, 5375–5384.

Tsuchiya M, Niwa Y, Simizu S (2016). *N*-glycosylation of R-spondin1 at Asn^{137} negatively regulates its secretion and Wnt/β-catenin signaling. Oncol Lett (*in press*).

Veeman MT, Slusarski DC, Kaykas A, Louie SH, Moon RT (2003). Zebrafish prickle, a modulator of noncanonical Wnt/Fz signaling, regulates gastrulation movements. Curr Biol 13, 680–685.

Wang D, Huang B, Zhang S, Yu X, Wu W, Wang X (2013). Structural basis for R-spondin recognition by LGR4/5/6 receptors. Genes Dev 27, 1339–1344.

Wang LW, Leonhard-Melief C, Haltiwanger RS, Apte SS (2009). Post-translational modification of thrombospondin type-1 repeats in ADAMTS-like 1/punctin-1 by *C*-mannosylation of tryptophan. J Biol Chem 284, 30004–30015.

Willert K, Brown JD, Danenberg E, Duncan AW, Weissman IL, Reya T, Yates JR 3rd, Nusse R (2003). Wnt proteins are lipid-modified and can act as stem cell growth factors. Nature 423, 448–452.

Yasukagawa T, Niwa Y, Simizu S, Umezawa K (2012). Suppression of cellular invasion by glybenclamide through inhibited secretion of platelet-derived growth factor in ovarian clear cell carcinoma ES-2 cells. FEBS Lett 586, 1504–1509.

Zeng YC, Lehrman MA (1990). A block at $Man_5GlcNAc_2$-pyrophosphoryldolichol in intact but not disrupted castanospermine and swainsonine-resistant Chinese hamster ovary cells. J Biol Chem 265, 2296–2305.